A Novel Soft-start Method for SVG Based on D-axis Orientation*

Shicheng Zheng[1, 2*], *Ying Shu*[1, 2], *Mengmeng Qi*[1, 2], *Jiahong Lang*[1, 2] *and Xuefeng Hu*[1, 2]
(1. School of Electrical and Information Engineering, Anhui University of Technology, Ma'anshan 243002, China;
2. Key Lab of Power Electronics & Motion Control, Anhui University of Technology, Ma'anshan 243002, China)

Abstract: In this paper, a novel method for shock-free soft-start is proposed. The novel method can realize the aim of no-overshoot and inrush of current during the entire soft-start process, thus the start process is safe, stable, and reliable. When the uncontrolled rectification stage ends, a sinusoidal signal synchronized with the grid voltage is generated through dq coordinate transformation and D-axis orientation, then the signal is transmitted to the three-phase inverter bridge. The AC voltage output of the inverter bridge is superimposed on both ends of the soft-start resistor along with the grid. The open-loop control method is adopted to gradually reduce the modulation ratio of the sinusoidal PWM wave until the capacitor voltage on the DC side reaches the rated voltage value, then the soft-start resistor is removed, which means the shock-free soft-start process is completed. Experimental results prove the effectiveness and feasibility of the control strategy proposed in this paper.

Keywords: Soft-start, coordinate transformation, modulation ratio, shock-free, D-axis orientation

1 Introduction

At present, due to the existence of a large number of non-linear, impulsive, and fluctuating loads in industrial production, increasingly serious power quality problems are brought to the power grid, which could potentially threaten the normal operation of power systems and user equipment [1]. Therefore, the power system puts forward the policy of "client power quality on-site compensation," requiring users to configure corresponding power quality detection and treatment equipment on the load side to eliminate the influence of these loads pollution [2]. Reactive power compensation technology has always been a research hotspot in the field of electrical engineering, whose function is to suppress the unbalanced grid voltage [3-4].

The static var generator (SVG) is a power electronic equipment connected in parallel to a common connection point, which is usually used to compensate the reactive power of the load and adjust the amplitude of the grid voltage by controlling the reactive power [5-7]. Compared with the static var compensator (SVC), which is a dynamic reactive power compensator, the SVG is widely used in improving the power quality due to its advantages, such as fast compensation time and continuous compensation. Therefore, SVG is currently a better way to solve the above-mentioned client power quality problem [8-10].

In Ref. [11], the D-axis orientation principle of SVG is proposed, which is used to ensure that the magnitude and phase of the SVG output voltage are consistent with the grid voltage. However, the current shock caused by the charging process of the starting capacitor was not analyzed. In Ref. [12], by increasing the p and q axis reference currents of the power grid, a new soft-start method for the grid-connected inverter was applied to prevent the current shock. However, the output current under this method fluctuates greatly.

SVG is basically controlled by fully controlled devices (IGBT) and pulse width modulation (PWM) control. During the start-up process of low-voltage control, the inductance of reactor connected between

Manuscript received October 14, 2020; revised December 15, 2020; accepted March 1, 2021. Date of publication March 31, 2021; date of current version March 8, 2021.
* Corresponding Author, E-mail: ahutzsc@126.com
* Supported by the Natural Science Foundation of Anhui Province (KJ2017A044).
Digital Object Identifier: 10.23919/CJEE.2021.000005

the inverter and grid is small, and there is a larger capacitor on the DC side, so a large starting surge current will be generated when the equipment is directly launched without control. As a result, there will be starting failure for the electrical and mechanical shocks caused by the starting current. More seriously, the equipment could also be damaged. Soft-start is a key technology to restrain unfavorable factors such as current impact and DC side voltage overcharge during the starting process, ensuring that the equipment can be started stably and put into operation smoothly. Therefore, soft-start technology is significant and difficult in the design of low-voltage SVG systems [13].

Hence, this paper proposes a new open-loop soft-start method based on the D-axis orientation, which not only realizes the non-impact soft-start of SVG, but also reduces the difficulty of debugging, while being easily implemented.

2 Topology and principle of SVG

The topology of the system is shown in Fig. 1. The voltage voltage-source type three-phase bridge converter circuit is composed of IGBTs installed in parallel on the load side through series reactors, and the dynamic compensation of reactive power could be realized according to the actual load [14-15]. Its principle can be illustrated by the single-phase equivalent circuit and vector diagram, which are shown in Fig. 2.

Defining the no-load phase voltage generated by the equipment as $\dot{U}_N$, the single-phase grid voltage as $\dot{U}_S$, the connected reactor equation as $jX = j\omega L$, and R as the equivalent resistor considering the loss of the connected reactor and converter. From Kirchhoff' s voltage law

$$\dot{U}_S = (R + j\omega L)\dot{I} + \dot{U}_I = \dot{U}_L + \dot{U}_I \tag{1}$$

where $\dot{U}_L$ is the voltage of the connected reactor, that is, the vector difference between $\dot{U}_S$ and $\dot{U}_I$; I is the current flowing through the reactor, which is also the compensation current of SVG. As shown in Fig. 2a, the output reactive power can be adjusted by controlling $\dot{U}_I$, which means that when the amplitude of $\dot{U}_I$ is greater than $\dot{U}_S$ and the phase of $\dot{U}_I$ lags $\dot{U}_S$, the phase of the compensation current $\dot{I}$ leads the grid voltage. The system will absorb the capacitive reactive power and show capacitive characteristics. When the amplitude of $\dot{U}_I$ is smaller than grid voltage $\dot{U}_S$ and the phase of $\dot{U}_I$ leads $\dot{U}_S$, the phase of the compensation current $\dot{I}$ lags the grid voltage. At this moment, the system will absorb inductive reactive power and show inductive characteristics. Therefore, the amplitude and performance of the compensation current of SVG can be changed by adjusting the magnitude and phase of the AC side voltage $\dot{U}_I$, and then the reactive power compensation can be achieved. As shown in Fig. 2b, due to the existence of loss, the error angle δ of the phase angle between grid voltage $\dot{U}_S$ and current $\dot{I}$ is smaller than 90°. Compared with the grid voltage, there exists active power in the current $\dot{I}$, which means that all the active losses of the equipment are provided by the power grid [16-17].

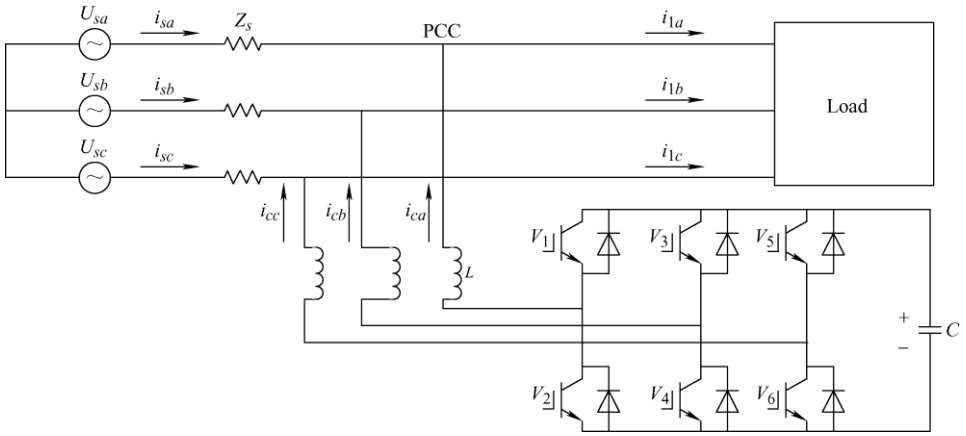

Fig. 1 System topology

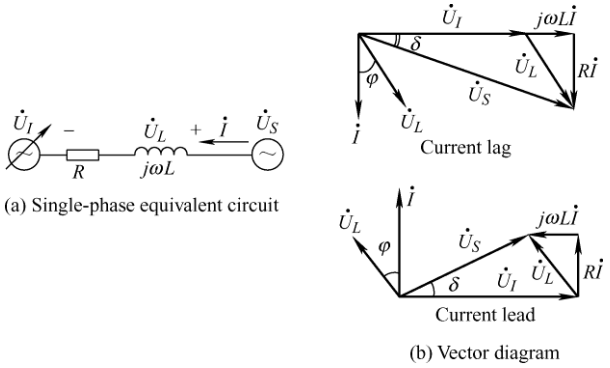

Fig. 2 Equivalent circuit and vector diagrams

As shown in Fig. 2b, when only the fundamental component is considered, taking the current $\dot{I}$ lagging the grid voltage $\dot{U}_S$ as an example, according to the vector triangle composed by the AC side voltage $\dot{U}_I$, the grid voltage $\dot{U}_S$, and the connected reactor voltage $\dot{U}_L$, then Eq. (2) could be written as

$$\frac{U_L}{\sin\delta}=\frac{U_I}{\sin\left(90^\circ-\varphi-\delta\right)}=\frac{U_S}{\sin\left(90^\circ+\varphi\right)} \tag{2}$$

where φ is the impedance angle of the connected reactor, δ is the phase error of $\dot{U}_S$ and $\dot{U}_I$. δ is positive when $\dot{U}_S$ lags $\dot{U}_I$. Then, Eq. (3) can be calculated as

$$U_L=U_S\frac{\sin\delta}{\sin(90^\circ+\varphi)}=U_S\frac{\sin\delta}{\cos\varphi} \tag{3}$$

The compensation current *I* can be calculated by the impedance value of the connected reactor ($Z=\sqrt{R^2+(\omega L)^2}$). Simultaneously, considering that the phase error of the current $\dot{I}$ and grid voltage $\dot{U}_S$ is $90^\circ-\delta$, and the projection of the current $\dot{I}$ on voltage $\dot{U}_S$ and its normal is the active and reactive current component absorbed by SVG, respectively, the effective values are

$$I_P=I\cos(90^\circ-\delta)=\frac{U_L}{\sqrt{R^2+(\omega L)^2}}\cos(90^\circ-\delta)=\frac{U_S}{2R}(1-\cos2\delta) \tag{4}$$

$$I_Q=I\sin(90^\circ-\delta)=\frac{U_L}{\sqrt{R^2+(\omega L)^2}}\sin(90^\circ-\delta)=\frac{U_S}{2R}\sin2\delta \tag{5}$$

From Eq. (2), the effective value of the AC side fundamental voltage of SVG is

$$U_I=U_S\frac{\sin(90^\circ-\varphi-\delta)}{\sin(90^\circ+\varphi)}=U_S\frac{\cos(\varphi+\delta)}{\cos\varphi} \tag{6}$$

From Eqs. (5) and (6), when the absolute value of the phase error δ is not too large, the effective value of the reactive current is approximately proportional to δ, and the effective value of the fundamental voltage on the AC side is also consistent with δ. Therefore, the amplitude and performance of the output current can be controlled by adjusting δ, then the reactive power can be adjusted continuously and quickly.

3 Soft-start strategy

3.1 Traditional strategy

In order to reduce the starting inrush current, many typical control methods have been employed to improve the system performance. But these methods are based on the following premise: the soft-start resistor is removed when the pre-charge ends and the PWM rectification method based on the closed-loop control is used to complete the soft-start of the DC side voltage. The equivalent schematic diagram of the device is shown in Fig. 3, where the output of the inverter is connected to the power grid through a reactor, a soft-start resistor, a contactor, and a circuit breaker. The conventional starting method is to keep the soft-start contactor closed at the end of the uncontrolled rectification phase, then the soft-start resistor is shorted out, and the DC side voltage can reach the given value by using the closed-loop voltage control method, completing the soft-start process of the system [18-20].

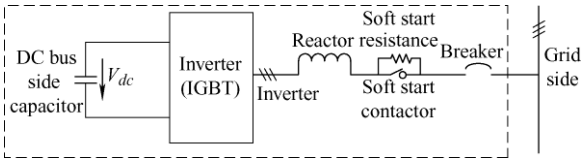

Fig. 3 Equivalent diagram of SVG

However, it can be seen from Fig. 3 that when the soft-start contactor is closed, the inverter starts to send out the PWM signal, due to the influence of dead zone and other factors, the output voltage of the inverter is smaller than the grid voltage. The soft-start resistor has been removed at this time, so that a voltage difference

will be generated on the connected reactor. As the inductive impedance of the reactor is very small, this voltage difference will generate a large surge current at the moment of switching, which will threaten the safety of power devices and eventually lead to the soft-start failure of the system. In addition, parameter tuning using the closed-loop PI control strategy is also difficult, which is not conducive to soft-start debugging.

3.2 Principle of D-axis orientation

In this paper, the open-loop soft-start control method with resistor based on D-axis orientation of the grid voltage is proposed to solve the problem that has been discussed above. The schematic diagram of coordinate transformation ($abc/\alpha\beta/dq$) is shown in Fig. 4.

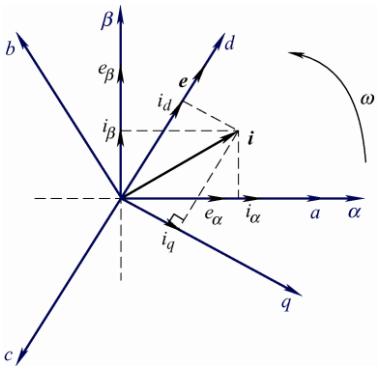

Fig. 4 Schematic diagram of coordinate transformation ($abc/\alpha\beta/dq$)

The transformation process is as follows: first, the instantaneous values of the three-phase grid voltage and current are transformed from the three-phase *abc* static coordinate system to the two-phase orthogonal $\alpha\beta$ static coordinate system through Clark transformation, and then further transformed to the synchronously rotating dq coordinate system by Park transformation.

The Clark transformation matrix and Park transformation matrix are respectively given by

$$\boldsymbol{C}_{abc/\alpha\beta}=\sqrt{\frac{2}{3}}\begin{bmatrix}1 & -\frac{1}{2} & -\frac{1}{2}\\ 0 & \frac{\sqrt{3}}{2} & -\frac{\sqrt{3}}{2}\end{bmatrix} \tag{7}$$

$$\boldsymbol{C}_{\alpha\beta/dq}=\begin{bmatrix}\sin\omega t & -\cos\omega t\\ -\cos\omega t & -\sin\omega t\end{bmatrix} \tag{8}$$

Therefore, Eq. (9) could be deduced as

$$\boldsymbol{C}_{abc/dq}=\boldsymbol{C}_{abc/\alpha\beta}\boldsymbol{C}_{\alpha\beta/dq}=\sqrt{\frac{2}{3}}\begin{bmatrix}\sin\omega t & \sin(\omega t-\frac{2\pi}{3}) & \sin(\omega t+\frac{2\pi}{3})\\ -\cos\omega t & -\cos(\omega t-\frac{2\pi}{3}) & -\cos(\omega t+\frac{2\pi}{3})\end{bmatrix} \tag{9}$$

After the coordinate transformation, the three-phase voltage signal of the power grid is transformed into the *d*-axis and *q*-axis components, which represent the active and reactive components, respectively.

In Fig. 4, the α-axis of the $\alpha\beta$ stationary coordinate system and the A-axis of the three-phase *abc* static coordinate system coincide with each other, and the rotation vector $\boldsymbol{e}$ in the α-β plane is composed of e_α and e_β. The counterclockwise rotation angular speed of $\boldsymbol{e}$ in space is ω. However, the dq coordinate system is a synchronous rotating coordinate system, and its angular velocity is also ω. By using the phase-locked control method, the *d*-axis could overlap with the rotation vector $\boldsymbol{e}$, that is, the D-axis orientation is realized. Simultaneously, the frequency and phase of the fundamental voltage output by the inverter side of the IGBT inverter bridge are completely identical to the grid voltage.

3.3 Analysis of the PWM boost rectification process

The open-loop voltage control is applied in the D-axis orientation soft-start stage. The equivalent schematic diagram of the AC side with a soft-start resistor for PWM rectification is shown in Fig. 5, where R is the sum of the soft-start resistor and the circuit equivalent resistor, X_L represents the equivalent impedance of the reactor, U_I represents the output voltage of the three-phase inverter side, and U_S represents the grid voltage. At the soft-start stage, the soft-start resistor is still connected in series in the circuit, therefore the amplitude of the grid voltage is higher than the inverter side, and the current I flows out of the power grid, which indicates the power grid is delivering power to the inverter side.

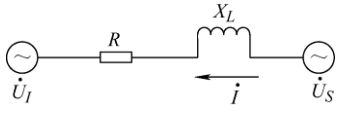

Fig. 5 Equivalent schematic diagram of the AC side

Fig. 6 shows the vector diagram of the AC side voltage with a soft-start resistor for PWM rectification, where U_I represents the output voltage of the

three-phase inverter side, U_S represents the grid voltage, U_R is the voltage drop across the circuit resistor, U_L is the voltage drop across the reactor, and θ is the angle between the current and the grid voltage, that is, the power factor angle.

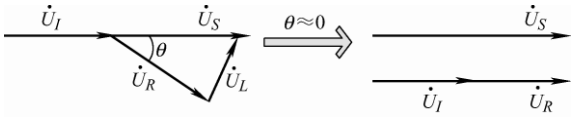

Fig. 6 Vector diagram of the AC side voltage at the soft-start stage

The expression for the power factor angle θ could be written as

$$\theta = \arctan\frac{\omega L}{R} \tag{10}$$

Compared with the equivalent resistor R, the equivalent impedance of the reactor is very small, and $\theta \approx 0$. It can be seen from Fig. 6 that the power grid is approximately at the state of unity power factor, which means almost all the active power of the grid is used to charge the DC side capacitor.

Simultaneously, when the modulation ratio is set to a maximum value close to 1 (such as 0.99), the phase and amplitude of the output voltage of the inverter side U_I is consistent with the grid voltage Us. Even if when the output voltage of the inverter side U_I is slightly smaller than the grid voltage U_S due to factors such as device voltage drop and dead zone, the existence of the soft-start resistor and the resistor is much greater than the equivalent impedance of the connected reactor, therefore, there is no current surge in the system.

Next, the modulation ratio M of the PWM wave is gradually reduced according to the step size ΔM shown in Eq. (11) at fixed intervals.

$$M = M - \Delta M \tag{11}$$

where ΔM is the step size, and the fixed intervals and ΔM depend on the interrupt period and the soft-start resistor. When the output voltage of the inverter side U_I drops, the capacitor voltage on the DC side will gradually increase to the rated voltage. The principle could be described as follows

$$U_{dc}(t) = U_{dc}(0) + \frac{1}{C}\int i\mathrm{d}t \tag{12}$$

$$U_{uv} = \frac{\sqrt{3}}{2}M \cdot U_{dc} \Rightarrow U_{dc} = \frac{2U_{uv}}{\sqrt{3}M} \tag{13}$$

where U_{uv} is the output line voltage of the three-phase inverter bridge and U_{dc} is the DC side capacitor voltage.

It can be seen from Eqs. (12) and (13) that the voltage variation process of the DC side capacitor can be expressed as follows

$$\begin{aligned} &M = (M - \Delta M)\downarrow \Rightarrow U_{UV}\downarrow \Rightarrow i\uparrow \Rightarrow U_{dc}\uparrow \Rightarrow \\ &U_{UV}\uparrow \Rightarrow i\downarrow \Rightarrow AgainM\downarrow \Rightarrow \cdots \Rightarrow U_{dc}\uparrow = U_{giv} \end{aligned} \tag{14}$$

With the periodic decrease of the modulation ratio M, the DC side capacitor voltage U_{dc} is gradually increased until its value is equal to the rated voltage value U_{giv}.

This paper adopts the soft-start method based on D-axis orientation. After the uncontrolled rectification stage finishes, coordinate transformation is performed on the grid voltage signal. Through the D-axis orientation of the grid voltage, a sinusoidal PWM signal synchronized with the grid voltage signal is generated and used as a modulation wave. After modulation, the six-PWM waves are generated to drive the power devices, and then the inverter bridge will output the AC voltage synchronized with the grid voltage, it is superimposed on both ends of the soft-start resistor with the grid voltage. By using the open-loop control, the modulation ratio of the PWM wave is gradually reduced until the voltage of capacitor on the DC side reaches the rated value. At this time, the soft-start resistor is cut off, and the entire soft-start process is completed.

4 Experimental results

Based on the above theoretical analysis, a ±100 kVar SVG device is developed. The main and rear views of the SVG are shown in Fig. 7, where the soft-start resistor is shown in Fig. 7a.

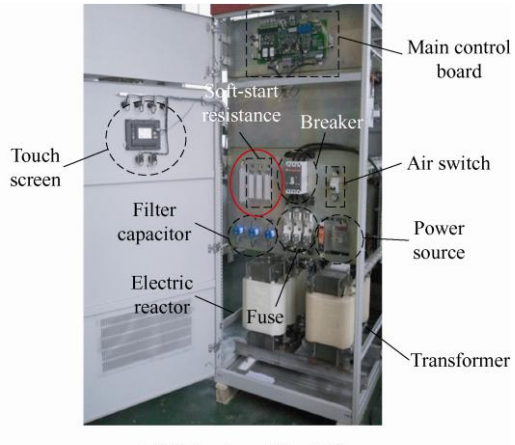

(a) Main view of the SVG

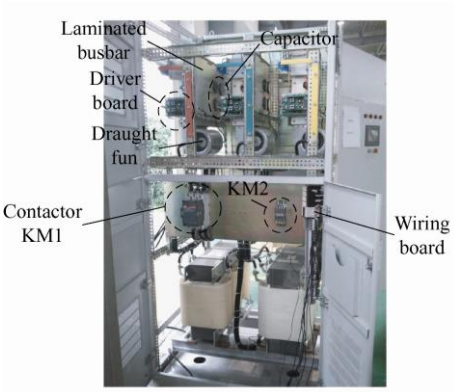

(b) Rear view of the SVG

Fig. 7 Experimental prototype platform of the SVG

The main parameters of the SVG are shown in Tab. 1.

Tab. 1 Main parameters of the SVG

Parameter	Value
Rated capacity Q/kVar	100
Operating voltage U_S/V	AC 380±15%
Rated compensation current I/A	225
Working frequency f_S/Hz	50±1
Response time T/ms	⩽5
Working mode	Automatic or manual
Operating display	Touch screen
Protection	Grid under-voltage, phase lack and phase dislocation, over-current, overheat, overvoltage and under-voltage of DC bus, overload automatic protection of current limit

Fig. 8 shows the soft-start waveform under the conventional soft-start method. Fig. 9 shows the soft-start waveform obtained under the method proposed in this paper. It can be seen from the experimental results that under the proposed method, the soft-start waveform rises more smoothly and has no overshoot.

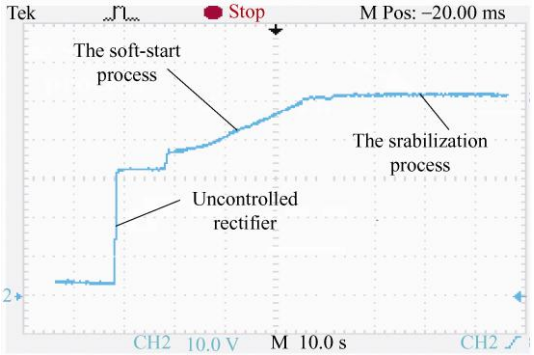

Fig. 8 Soft-start waveform under the conventional soft-start method

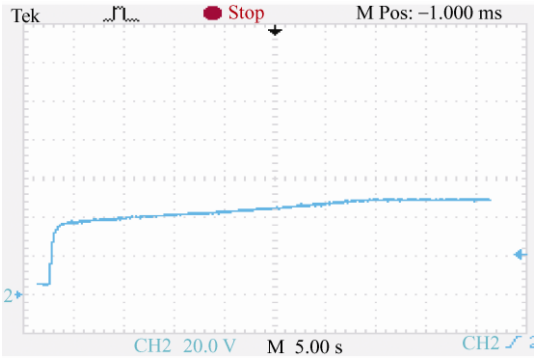

Fig. 9 Soft-start waveform obtained under the proposed soft-start method

In order to further verify the dynamic and steady performance of the SVG, a closed-loop grid-connected experiment is carried out. The voltage and current waveforms of phase A of the grid side at steady state is shown in Fig. 10.

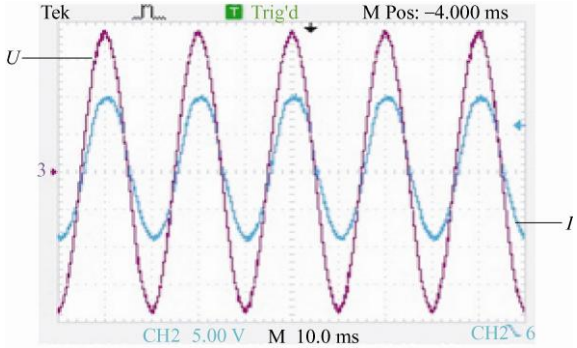

Fig. 10 Voltage and current waveforms of phase A of the grid side

As shown in Fig. 10, the phases of the voltage and current are consistent, and it can be concluded that the SVG has achieved unity power factor control. Fig. 11 shows the experimental waveforms under different load conditions. It can be seen from the figure that the system can quickly track the change of the reactive current signal on the load side, and the phases of voltage and current are consistent during the entire soft-start process.

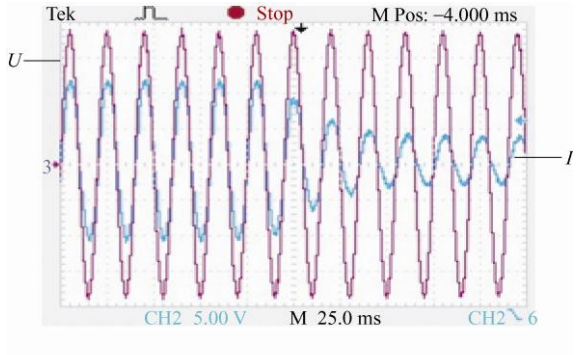

(a) Voltage and current waveforms when the load drops

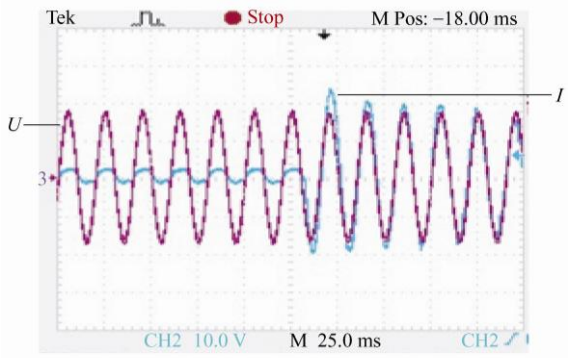

(b) Voltage and current waveforms when the load rises

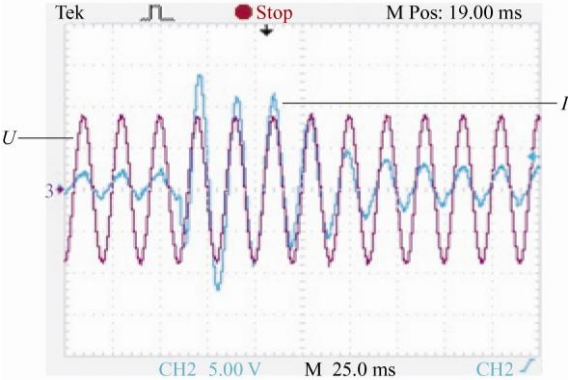

(c) Voltage and current waveforms under impactive load

Fig. 11 Experimental waveforms under different load conditions

5 Conclusions

This paper discusses a soft-start strategy used in SVG. The reason for the failure of traditional soft-start is analyzed and a novel SVG soft-start control strategy based on D-axis orientation is proposed. Through experiments, the soft-start waveforms under two methods are obtained, which are consistent with the theoretical analysis. The experimental results verify the validity and feasibility of the proposed scheme.

References

[1] L Liu, H Li, Y Xue, et al. Reactive power compensation and optimization strategy for grid-interactive cascaded photovoltaic systems. *IEEE Transactions on Power Electronics*, 2015, 30(1): 188-202.

[2] J Yi, W Hu, Z J Zhang, et al. Steady-state voltage reactive compensation method for half-wavelength transmission lines considering equivalent power supply impedance. *CSEE Journal of Power and Energy Systems*, 2020, 6(4): 841-847.

[3] L Wang, C Lam, M Wong. Selective compensation of distortion, unbalanced and reactive power of a thyristor-controlled LC-coupling hybrid active power filter (TCLC-HAPF). *IEEE Transactions on Power Electronics*, 2017, 32(12): 9065-9077.

[4] S X Chen, Y S F Eddy, H B Gooi, et al. A centralized reactive power compensation system for LV distribution networks. *IEEE Transactions on Power Systems*, 2015, 30(1): 274-284.

[5] Y He, W Duan, Y Fu. Research on DC voltage balancing control method of star connection cascaded H-bridge static var generator. *IET Power Electronics*, 2016, 9(7): 1505-1512.

[6] S Zheng, Z Li, M Cao. Direct current control strategy of SVG based on dual sequence dq coordinates under asymmetric load condition. *Chinese Journal of Electrical Engineering*, 2019, 5(1): 24-35.

[7] K J Lee, B G Park, R Y Kim. Robust predictive current controller based on a disturbance estimator in a three-phase grid-connected inverter. *IEEE Transaction on Power Electronics*, 2012, 27(1): 276-283.

[8] Y Wan, M A A Murad, M Liu, et al. Voltage frequency control using SVC devices coupled with voltage dependent loads. *IEEE Transactions on Power Systems*, 2019, 34(2): 1589-1597.

[9] S Das, D Chatterjee, S K Goswami. Tuned-TSC based SVC for reactive power compensation and harmonic reduction in unbalanced distribution system. *IET Generation, Transmission & Distribution*, 2017, 12(3): 571-585.

[10] X Wang, L Xu, P Fu, et al. Operation analysis and improvement of impulse current test on high-power DC test platform with SVC system. *IEEE Transactions on Plasma Science*, 2018, 46(5): 1658-1664.

[11] J J Liu. The research and design of static var generator (SVG). Tianjin: Tianjin University of Technology, 2012.

[12] Z L Yao, L Xiao. Soft-start control for SVPWM-based three-phase grid-connected inverters. *High Voltage Engineering*, 2013, 39(11): 2750-2755.

[13] Z Yao. Soft-start control strategy for the three-phase grid-connected inverter with LCL filter. *Electronics Letters*, 2016, 52(14): 1242-1244.

[14] P Liu, C Hsu, Y Chang. Techniques of dual-path error amplifier and capacitor multiplier for on-chip compensation and soft-start function. *IEEE Transactions on Power Electronics*, 2015, 30(3): 1403-1410.

[15] L Zhu, X Chen. An investigation of a novel snapback-free reverse-conducting IGBT and with dual gates. *IEEE Transactions on Electron Devices*, 2012, 59(11): 3048-3053.

[16] Q P Xiong, A Luo. A single-carrier modulation strategy for cascade SVG. *Chinese Society for Electrical Engineering*, 2013, 33(24): 74-81.

[17] G Cao, K Sun, S Jiang, et al. A modular DC/DC

photovoltaic generation system for HVDC grid connection. *Chinese Journal of Electrical Engineering,* 2018, 4(2): 56-64.

[18] H Lu, Q J Wang. Soft-start of three-phase photovoltaic inverter based on modified segmentation fuzzy control. *Power Electronics*, 2015, 49(6): 74-77.

[19] S Fan, Z Xue, Z Guo, et al. VRSPV soft-start strategy and AICS technique for boost converters to improve the start-up performance. *IEEE Transactions on Power Electronics*, 2016, 31(5): 3663-3672.

[20] Y Lin, C Chen. Undershoot-less open-loop soft-start strategy for digital-controlled power converters based on an error-ADC and initial duty ratio estimator. *IEEE Transactions on Circuits and Systems II: Express Briefs*, 2019, 66(9): 1542-1546.

Shicheng Zheng received his Ph.D degree in electrical engineering from Hefei University of Technology (HFUT), Hefei, China, in 2005. In 2005, he joined the School of Electrical and Information Engineering at Anhui University of Technology, Ma'anshan, China, to undertake research in the area of power electronics and power drive. He was appointed lecturer in 2008. He is currently a professor in the School of Electrical and Information Engineering, Anhui University of Technology.

His current research interests focus on power converters, grid connected inverters, distributed power generation, power drive and power quality, and so on.

Professor Zheng is a senior member of the CPSS.

Ying Shu received her B.S. degree in electrical engineering from East China Jiaotong University, Nanchang, China, in 2018, where she is presently working towards her M.S. degree.

Her current research interests include power electronics, DC-DC power conversion, and the modeling and control of converters.

Mengmeng Qi received his B.S. degree in electrical engineering from Beihua University, Jilin, China, in 2019, where he is presently working towards his M.S. degree.

His current research interests include power electronics, DC-DC power conversion, and the modeling and control of converters.

Jiahong Lang received his B.S. degree in the Department of Physics, Anhui University, Hefei, China, in 1997, and the M.S degree in the Key Laboratory of Materials Modification by Laser, Ion and Electron Beams (Dalian University of Technology) Ministry of Education. He is currently an associate professor in the School of Electrical and Information Engineering, Anhui University of Technology, Ma'anshan, China.

His current research interests include power converters, automatic control system design, monitoring and optimization, new energy development technology, and power quality management.

Xuefeng Hu received the M.S. degree in electronic engineering from the China University of Mining and Technology, Xuzhou, China, in 2004, and the Ph.D. degree in electrical engineering from the Nanjing University of Aeronautics and Astronautics, Nanjing, China, in 2014. He is currently a professor at Anhui University of Technology, Ma'anshan, China. He is the author or co-author of more than 40 technical papers.

His current research interests include renewable energy systems, the modeling and control of converters, and flexible AC transmission systems.